

Symmetry–Protected Momentum Exchange between Dark Matter and Dark Energy

Mohid Farhan*

Department of Space Science, Institute of Space Technology, Islamabad, Pakistan

(Dated: March 10, 2026)

We present a particle–physics motivated realization of interacting dark energy in which a radiatively stable dark energy sector couples to weakly interacting massive particle dark matter through pure momentum exchange. The dark energy field arises as a pseudo–Nambu–Goldstone boson from a complex scalar singlet charged under a softly broken global $U(1)_S$, while dark matter is identified with an inert scalar doublet stabilized by a discrete Z_4 symmetry. This symmetry structure allows renormalizable dark matter–dark energy portal operators; however, requiring the dark energy field to emerge as a radiatively stable pseudo–Nambu–Goldstone boson necessitates their absence, leaving derivative interactions as the leading coupling. As a result, energy transfer between the dark sectors is absent at the background level, while momentum exchange modifies the evolution of cosmological perturbations. We implement the resulting interacting dark energy model self–consistently in the Boltzmann code CLASS and study its impact on the growth of structure. We find that, despite sizeable momentum exchange, the suppression of the clustering amplitude σ_8 saturates above the level required to fully resolve current low–redshift tensions. Our results demonstrate that symmetry–protected, momentum–exchange–only dark sector interactions possess an intrinsic limit on structure suppression, providing a theoretically controlled benchmark for interacting dark energy scenarios.

I. INTRODUCTION

The nature of dark matter (DM) and dark energy (DE) remains one of the central open problems in modern cosmology. While the Λ CDM paradigm successfully describes a wide range of cosmological observations, persistent tensions between early- and late-time measurements (most notably in the clustering amplitude σ_8 and the Hubble parameter H_0) have motivated the exploration of physics beyond a minimally coupled cosmological constant [1–3]. Among the proposed extensions, interacting dark energy (IDE) models provide a theoretically appealing framework in which non-gravitational interactions within the dark sector modify the growth of cosmic structure while leaving the visible sector largely unaffected.

A broad class of IDE scenarios introduces an explicit coupling between DM and DE through phenomenological energy transfer terms at the level of the cosmological continuity equations [4, 5]. While such models can alleviate certain observational tensions, they often lack a well-defined particle physics origin and may suffer from instabilities, strong coupling issues, radiative sensitivity or fine-tuning [6, 7]. These shortcomings have motivated the study of IDE models in which energy transfer vanishes at the background level, leaving only momentum exchange between the dark sectors [8–10]. Momentum-exchange IDE models are known to affect cosmological perturbations without altering the background expansion history, making them particularly attractive from an observational consistency standpoint.

Despite their phenomenological appeal, most momentum-exchange IDE models are formulated at the level of effective fluids or phenomenological drag

terms, with limited connection to an underlying ultraviolet-complete theory. Embedding such interactions into a consistent particle physics framework poses significant challenges, especially when dark energy is dynamical. In particular, any viable DE scalar field must remain radiatively stable against large quantum corrections, which generically drive its mass far above the Hubble scale unless protected by a symmetry [11, 12].

A well-known mechanism to stabilize ultralight scalar fields is to realize dark energy as a pseudo–Nambu–Goldstone boson (pNGB) associated with the spontaneous breaking of a global symmetry [13, 14, 40]. In such constructions, the shift symmetry of the pNGB protects the scalar mass, while soft symmetry breaking generates a naturally small potential. Separately, inert scalar extensions of the Standard Model provide a minimal and well-studied framework for weakly interacting massive particle (WIMP) dark matter, stabilized by a discrete symmetry and compatible with collider, astrophysical, and cosmological constraints [15–17].

In this work, we combine these two ideas into a unified, symmetry-protected dark sector in which a pNGB dark energy field interacts with inert scalar dark matter exclusively through momentum exchange. The dark energy sector arises from a complex scalar singlet charged under a global $U(1)_S$ symmetry that is spontaneously broken at a high scale and softly broken by a dimension-two operator, ensuring radiative stability of the pNGB mass. Dark matter is identified with an inert scalar doublet stabilized by a discrete Z_4 symmetry. Crucially, while the imposed symmetry structure allows renormalizable dark matter–dark energy portal operators, the requirement that dark energy emerge as a radiatively stable pseudo–Nambu–Goldstone boson necessitates their absence, leaving derivative interactions as the leading coupling. As a consequence, energy transfer between dark matter and dark energy vanishes

* mohid35@gmail.com

at the background level, while momentum exchange modifies the evolution of cosmological perturbations.

We implement this interacting dark energy model self-consistently in the Boltzmann code CLASS and study its impact on the growth of large-scale structure. Our analysis demonstrates that, even for sizeable momentum-exchange rates, the suppression of σ_8 saturates above the level required to fully resolve current low-redshift tensions. This result indicates that symmetry-protected, momentum-exchange-only dark sector interactions possess an intrinsic limit on their ability to suppress structure growth.

The purpose of this paper is twofold. First, we provide an explicit particle physics realization of momentum-exchange interacting dark energy that is radiatively stable and symmetry controlled. Second, we use this framework to assess the extent to which such interactions can impact cosmological observables, thereby clarifying the capabilities and limitations of this class of models. Our results establish a theoretically well-motivated benchmark for interacting dark energy scenarios and provide guidance for future extensions involving additional interactions or symmetry breaking effects.

II. THEORETICAL FRAMEWORK

Field Content and Symmetries

We consider an extension of the Standard Model (SM) featuring an inert scalar doublet and a complex scalar singlet, which together constitute the dark sector [15–17]. The field content is

$$H = \begin{pmatrix} H_1^+ \\ \frac{H_1^0 + iA_1^0}{\sqrt{2}} \end{pmatrix}, H_2 = \begin{pmatrix} H_2^+ \\ \frac{H_2^0 + iA_2^0}{\sqrt{2}} \end{pmatrix}, S = \left(\frac{v_s + \rho + i\phi}{\sqrt{2}} \right). \quad (1)$$

where H is the SM Higgs doublet, H_2 is an inert scalar doublet identified with dark matter, and S is a complex scalar singlet responsible for dark energy [18].

The theory is endowed with a discrete Z_4 symmetry and a global $U(1)_S$ symmetry under which the fields transform as

$$H \rightarrow H, \quad H_2 \rightarrow -H_2, \quad S \rightarrow iS, \quad S \rightarrow e^{i\alpha}S. \quad (2)$$

The Z_4 symmetry stabilizes the inert scalar doublet and ensures the absence of dark matter decay into Standard Model states [19]. However, the $Z_4 \times U(1)_S$ symmetry alone does not forbid all renormalizable interactions between the inert doublet and the singlet sector. In particular, operators of the form $|S|^2|H_2|^2$ are invariant under both symmetries and would generically be allowed [20].

The absence of such operators in the present framework is enforced by the requirement that the dark energy field emerge as a pseudo-Nambu-Goldstone boson with a radiatively stable, ultralight mass [13, 14].

This necessitates that the global $U(1)_S$ symmetry be spontaneously broken by the singlet vacuum expectation value while being only *softly* broken in the potential [21, 22]. The soft breaking is achieved through a single dimension-two operator proportional to μ_{sb}^2 , which is the unique source of explicit symmetry violation in the singlet sector [23]. Consequently, any interaction that would generate an unsuppressed mass for the angular mode ψ must be set to zero in order to preserve the pNGB nature of dark energy. Their vanishing protects the technical naturalness of the pNGB mass scale, though as we shall see, this is a phenomenological requirement rather than a symmetry-enforced selection [11, 12].

Expanding the singlet field around its vacuum expectation value,

$$\langle S \rangle = \frac{v_s}{\sqrt{2}}, \quad S = \frac{1}{\sqrt{2}}(v_s + \rho + i\phi), \quad (3)$$

the angular mode ϕ transforms nonlinearly under $U(1)_S$ and is identified with the dark energy field [24]. At tree level, its mass is controlled entirely by the soft-breaking parameter,

$$m_\phi^2 = 2|\mu_{sb}^2|, \quad (4)$$

while the radial mode acquires a mass $m_\rho^2 = \lambda_S v_s^2 + 2|\mu_{sb}^2| \approx \lambda_S v_s^2$. In the limit $\mu_{sb}^2 \rightarrow 0$, the $U(1)_S$ symmetry is restored and the dark energy field becomes exactly massless. The smallness of $m_\phi \sim H_0$ is therefore technically natural: it is protected from large radiative corrections by the fact that μ_{sb}^2 is the only explicit breaking parameter, and any correction to m_ϕ^2 must be proportional to μ_{sb}^2 itself [21].

Scalar Potential and Symmetry Structure

The most general renormalizable scalar potential consistent with gauge symmetry and the imposed $Z_4 \times U(1)_S$ charges contains all allowed operators:

$$\begin{aligned} V(H, H_2, S) = & \mu_1^2 |H|^2 + \mu_2^2 |H_2|^2 + \mu_S^2 |S|^2 \\ & + \frac{\lambda_1}{2} |H|^4 + \frac{\lambda_2}{2} |H_2|^4 + \frac{\lambda_S}{2} |S|^4 \\ & + \lambda_3 |H|^2 |H_2|^2 + \lambda_4 |H^\dagger H_2|^2 + \left[\frac{\lambda_5}{2} (H^\dagger H_2)^2 + \text{h.c.} \right] \\ & + \lambda_{S1} |S|^2 |H|^2 + \lambda_{S2} |S|^2 |H_2|^2 \\ & + [\lambda_{S12} S^2 (H^\dagger H_2) + \lambda_{S21} S^{*2} (H^\dagger H_2) + \text{h.c.}] \\ & + [\lambda_{S4} S^4 + \text{h.c.}] + \left[\frac{\mu_{sb}^2}{2} S^2 + \text{h.c.} \right], \quad (5) \end{aligned}$$

where all portal couplings ($\lambda_{S1}, \lambda_{S2}, \lambda_{S12}, \lambda_{S21}, \lambda_{S4}$) are invariant under Z_4 and $U(1)_S$, and μ_{sb}^2 parametrizes the soft breaking.

However, the portal operators $|S|^2|H_2|^2$ and $|S|^2|H|^2$ are incompatible with the pseudo-Nambu-Goldstone nature of dark energy. When S acquires its vacuum

expectation value, these terms contribute to the Coleman-Weinberg potential for the angular mode ϕ [25], generating a mass-squared correction at one-loop order. The dominant contribution arises from the dark matter loop, giving

$$\delta m_\phi^2 = \frac{\lambda_{S2}^2}{16\pi^2} m_{H_2}^2 \left[\ln \left(\frac{\Lambda^2}{m_{H_2}^2} \right) + \mathcal{O}(1) \right], \quad (6)$$

where Λ denotes the ultraviolet cutoff scale. Renormalization group analysis of the IDSM reveals that the model loses perturbativity at $\Lambda \sim 10^8$ GeV due to the running of the inert doublet couplings. Requiring that the quantum correction not exceed the tree-level mass, $|\delta m_\phi^2| \leq m_\phi^2 = 2|\mu_{sb}^2|$, imposes the constraint

$$\lambda_{S2}^2 \leq \frac{16\pi^2 m_\phi^2}{m_{H_2}^2 \ln(\Lambda^2/m_{H_2}^2)}. \quad (7)$$

For a weak-scale dark matter particle with $m_{H_2} \sim 10^2$ GeV and dark energy mass $m_\phi \sim H_0 \sim 10^{-33}$ eV $\sim 10^{-42}$ GeV, taking $\Lambda \sim 10^8$ GeV yields $\ln(\Lambda^2/m_{H_2}^2) \sim 28$ and

$$|\lambda_{S2}| \lesssim \frac{4\pi \times 10^{-42} \text{ GeV}}{(10^2 \text{ GeV}) \times \sqrt{28}} \sim 10^{-44}. \quad (8)$$

The operators $S^2(H^\dagger H_2)$ and $S^{*2}(H^\dagger H_2)$ similarly contribute to the ϕ mass through mixing with the radial mode ρ at comparable levels, while S^4 contributes to the Coleman-Weinberg potential for ρ and indirectly to ϕ after symmetry breaking. All these effects would destroy the hierarchy between the dark energy scale and the electroweak scale [26]. We therefore impose the **pNGB protection condition**: all hard portal couplings between the singlet and doublet sectors are set to zero:

$$\lambda_{S1} = \lambda_{S2} = \lambda_{S12} = \lambda_{S21} = \lambda_{S4} = 0. \quad (9)$$

The sole remnant of explicit breaking in the singlet sector is the soft term μ_{sb}^2 . This choice is motivated by naturalness: it protects the ultralight mass of the dark energy field from quantum corrections proportional to the heavy scales in the dark matter sector [21]. However, it is *not enforced by the $Z_4 \times U(1)_S$ symmetry*—the symmetry structure allows these operators; their absence should be understood as a phenomenological boundary condition necessary for a viable quintessence scenario [11].

The resulting potential, which we denote V_{sym} , then separates into minimal and decoupled sectors:

$$\begin{aligned} V_{\text{sym}} = & \mu_1^2 |H|^2 + \mu_2^2 |H_2|^2 + \frac{\lambda_1}{2} |H|^4 + \frac{\lambda_2}{2} |H_2|^4 + \lambda_3 |H|^2 |H_2|^2 \\ & + \lambda_4 |H^\dagger H_2|^2 + \left[\frac{\lambda_5}{2} (H^\dagger H_2)^2 + \text{h.c.} \right] \\ & + \mu_S^2 |S|^2 + \frac{\lambda_S}{2} |S|^4 + \left[\frac{\mu_{sb}^2}{2} S^2 + \text{h.c.} \right]. \end{aligned} \quad (10)$$

We require $\mu_S^2 < 0$ to spontaneously break $U(1)_S$, giving S a VEV.

Radiative Stability and Renormalization Group Considerations

The radiative isolation of the dark energy sector is verified through the one-loop renormalization group equations. In the pNGB-protected limit where all singlet-doublet portal couplings vanish, the β -functions for the singlet mass parameters receive no contributions from the Higgs or inert doublet sectors:

$$16\pi^2 \beta_{\mu_S^2} = 4\lambda_S \mu_S^2, \quad 16\pi^2 \beta_{\mu_{sb}^2} = 2\lambda_S \mu_{sb}^2. \quad (11)$$

The absence of terms involving μ_1^2 , μ_2^2 , $\lambda_{3,4,5}$, or gauge/Yukawa couplings confirms that the electroweak scale does not destabilize the singlet sector [22]. This radiative isolation is a direct consequence of the imposed symmetries and the pNGB protection condition.

The complete one-loop RGEs for the model are summarized in Table II (see Appendix A). The decoupling of the singlet sector from SM running ensures that the smallness of μ_{sb}^2 is preserved under RG evolution, with corrections proportional only to μ_{sb}^2 itself [23].

This framework therefore provides a consistent ultraviolet-motivated realization of momentum-exchange interacting dark energy. The absence of renormalizable energy-transfer operators—enforced by the pNGB protection condition rather than by fine-tuning—distinguishes this construction from conventional phenomenological IDE models [4, 5], while the derivative nature of the leading interaction ensures background stability [8–10].

Leading Derivative Interaction and Momentum Exchange

Although renormalizable portals are absent, higher-dimensional operators consistent with the symmetries are generically expected to arise after integrating out heavy degrees of freedom [27]. The leading interaction between dark matter and dark energy appears at dimension six and takes the schematic form [8, 9]

$$\mathcal{L}_{\text{int}} = \frac{c_6}{\Lambda^2} (\partial_\mu |S|^2) (\partial^\mu |H_2|^2), \quad (12)$$

where Λ denotes the effective cutoff scale and c_6 is a dimensionless coefficient.

After spontaneous symmetry breaking and integrating out the heavy radial mode ρ , this operator induces derivative couplings between the pNGB field ϕ and the inert scalar dark matter [10]. Importantly, such interactions do not contribute to the background energy-momentum transfer but instead generate a drag force at the level of perturbations [8]. The resulting cosmological dynamics correspond to a pure momentum-exchange interacting dark energy scenario, as studied phenomenologically in previous works [9, 10, 28].

III. METHODOLOGY

The analysis presented in this work combines particle-physics calculations of dark matter phenomenology with cosmological evolution at the level of linear perturbations. The two aspects are treated independently and then consistently interfaced. Dark matter properties are computed using the public code `micrOMEGAs`, while the impact of dark matter–dark energy momentum exchange on cosmological observables is evaluated using a modified version of the Boltzmann solver `CLASS`. Importantly, the background cosmological evolution remains unaltered relative to Λ CDM, and all modifications enter exclusively at the level of perturbations. We also derive an expression for the DM–DE drag rate Γ .

Dark Matter Phenomenology using `MicrOMEGAs`

The relic density Ωh^2 of the dark matter candidate is computed using `micrOMEGAs`, a numerical package designed to evaluate dark matter observables across BSM frameworks. For each model, the particle content and interactions are specified via model files in `CalcHEP` format [29, 30]. The time evolution of the dark matter number density n_χ is governed by the Boltzmann equation, which `micrOMEGAs` solves numerically:

$$\frac{dn_\chi}{dt} + 3Hn_\chi = -\langle\sigma v\rangle (n_\chi^2 - n_\chi^{\text{eq}2}), \quad (13)$$

where H is the Hubble parameter, $\langle\sigma v\rangle$ is the thermally averaged annihilation cross-section, and n_χ^{eq} is the equilibrium number density. `MicrOMEGAs` computes the thermally averaged cross-section using:

$$\langle\sigma v\rangle = \frac{1}{C_1} \int_{4m_\chi^2}^{\infty} ds \sigma(s) (s - 4m_\chi^2) \sqrt{s} K_1(\sqrt{s}/T), \quad (14)$$

where $C_1 = 8m_\chi^4 T K_2^2(m_\chi/T)$. K_1 and K_2 are modified Bessel functions, and $\sigma(s)$ includes all $2 \rightarrow 2$ annihilation and coannihilation channels. The relic abundance is derived via numerical integration over temperature:

$$\Omega_\chi h^2 = \frac{1.07 \times 10^9 \text{ GeV}^{-1}}{g_*^{1/2} M_{\text{Pl}} \int_{x_f}^{\infty} \frac{\langle\sigma v\rangle}{x^2} dx}, \quad (15)$$

where $x = m_\chi/T$, x_f is the freeze-out point, g_* denotes effective relativistic degrees of freedom, and M_{Pl} is the Planck mass. The relic density of dark matter is constrained to be in the region:

$$\Omega h^2 = 0.1199 \pm 0.0027 \quad (16)$$

by Planck data [1]. To maintain consistency with observation, we will include these bounds in our computational analysis.

Cosmological Perturbations with `CLASS`

We implement the Z_4 -IDS M cosmology in the `CLASS` (Cosmic Linear Anisotropy Solving System) code [31, 32], modifying the perturbation evolution to include momentum exchange between dark matter and the pNGB dark energy fluid. The implementation preserves the background evolution of standard Λ CDM while introducing drag terms in the perturbation equations [35]. We employ the Newtonian gauge throughout [36], with metric perturbations Ψ and Φ defined through the line element $ds^2 = a^2(\tau)[-(1 + 2\Psi)d\tau^2 + (1 - 2\Phi)\delta_{ij}dx^i dx^j]$.

The background module requires no modification. The dimension-6 operator contributes negligibly to the homogeneous energy density, ensuring that $\rho_{\text{DM}}(a)$ and $\rho_{\text{DE}}(a)$ evolve independently according to the standard continuity equations [8, 9]. The dark energy equation of state $w(a)$ is determined by the pNGB potential, which for the softly broken $U(1)_S$ takes the form of a shifted quadratic in the field displacement. The Hubble expansion $H(a)$ thus follows the standard Friedmann equation with uncoupled dark sectors at the background level.

The momentum exchange enters through modified Euler equations for the velocity divergences $\theta_{\text{cdm}} \equiv ik^i v_{\text{cdm},i}$ and $\theta_{\text{fld}} \equiv ik^i v_{\text{fld},i}$. In the Newtonian gauge, the cold dark matter velocity equation becomes

$$\theta'_{\text{cdm}} + \mathcal{H}\theta_{\text{cdm}} - k^2\Psi = a\Gamma(a)(\theta_{\text{fld}} - \theta_{\text{cdm}}), \quad (17)$$

where primes denote conformal time derivatives, $\mathcal{H} = aH$ is the conformal Hubble parameter, and $\Gamma(a)$ is the momentum-transfer rate. The dark energy fluid velocity equation acquires the opposite drag term weighted by the density ratio to ensure total momentum conservation [10, 28]:

$$\theta'_{\text{fld}} + \mathcal{H}(1 - 3c_s^2)\theta_{\text{fld}} - \frac{c_s^2}{1+w}k^2\delta_{\text{fld}} - k^2\Psi = aR_{\text{fld}}\Gamma(a)(\theta_{\text{cdm}} - \theta_{\text{fld}}), \quad (18)$$

where c_s^2 is the sound speed of the pNGB (typically $c_s^2 = 1$ for a canonical scalar field), and the weight factor

$$R_{\text{fld}} = \frac{\rho_{\text{cdm}}}{\rho_{\text{fld}}(1+w)} \quad (19)$$

ensures that the interaction conserves the total momentum density $\rho_{\text{cdm}}\theta_{\text{cdm}} + \rho_{\text{fld}}(1+w)\theta_{\text{fld}}$ up to Hubble drag terms.

From the dimension-6 operator $\mathcal{L}_{\text{int}} = (c_6/\Lambda^2)(\partial_\mu|S|^2)(\partial^\mu|H_2|^2)$, integrating out the heavy radial mode ρ yields the low-energy momentum-transfer rate

$$\Gamma(a) = \frac{c_6 v_s^2}{\Lambda^2 m_{H_2}^2} \rho_{\text{cdm}}(a) H(a) \equiv \xi H(a) \left[\frac{\rho_{\text{cdm}}(a)}{\rho_{\text{cdm},0}} \right], \quad (20)$$

where we have defined the dimensionless coupling parameter $\xi \equiv (c_6 v_s^2 / \Lambda^2 m_{H_2}^2) \rho_{\text{cdm},0} H_0$. This parametrization makes explicit that $\Gamma \sim H$ when the

coupling is order unity, and that the interaction strength grows with the dark matter density as expected for a contact interaction [41].

The modifications are implemented in the `perturbations.c` module of CLASS v3.0 [31, 37]. The new input parameters `c6` (dimensionless coupling constant), `vs2` (singlet VEV squared v_s^2 in GeV^2), `Lambda2` (cutoff scale squared Λ^2 in GeV^2), and `mH2_2` (inert doublet mass squared $m_{H_2}^2$ in GeV^2) are passed through the `perturbations_parameters_and_workspace` structure to the integration routines. The drag terms are added to the right-hand side of the linear perturbation system in the `perturbations_derivs()` function, evaluated at each time step alongside the standard Einstein-Boltzmann terms.

We disable the Parameterized Post-Friedmann (PPF) formalism [33, 34] by setting `use_ppf = no` in the parameter file. The PPF scheme replaces the explicit fluid velocity θ_{fld} with a single “slipping” variable Γ_{fld} , which is incompatible with our direct coupling between θ_{fld} and θ_{cdm} in Eq. (18). When PPF is active, `index_pt_theta_fld` is not allocated, causing segmentation faults upon accessing the velocity perturbation.

The system of differential equations is evolved using the NDF15 integrator [32], an implicit solver optimized for stiff equations that exhibits good performance even in the tight-coupling regime $\Gamma \gtrsim H$. However, when $\Gamma \gg H$, the strong coupling leads to rapid oscillations in the relative velocity ($\theta_{\text{cdm}} - \theta_{\text{fld}}$) that exhaust the adaptive step-size controller, resulting in “step size too small” errors. This defines the practical upper limit of the effective field theory. We find that stable integration requires $\xi \lesssim \mathcal{O}(10)$, corresponding to $\Gamma \lesssim 10H$ at $z \sim 0$.

The matter power spectrum $P(k)$ and CMB angular power spectra $C_\ell^{TT,TE,EE}$ are extracted using the standard CLASS output routines. The linear growth factor $f(z) \equiv d \ln D / d \ln a$ and the σ_8 normalization are computed from the matter power spectrum at $z = 0$ following the standard definitions [1].

Phenomenological Treatment of the DM–DE Drag Rate

The momentum-transfer rate $\Gamma(a)$ entering the cosmological perturbation equations originates from the dimension-6 interaction between the dark sectors. We outline the connection between the microscopic EFT and the macroscopic fluid description.

The lowest-dimensional operator capable of mediating DM–DE momentum exchange and consistent with the imposed $Z_4 \times U(1)_S$ symmetry is:

$$\mathcal{L}_{\text{int}} = \frac{c_6}{\Lambda^2} (\partial_\mu |S|^2) (\partial^\mu |H_2|^2), \quad (21)$$

where $c_6 \sim \mathcal{O}(1)$ is a Wilson coefficient and Λ denotes the EFT cutoff scale [8, 27]. At energies $E \ll m_\rho$, this

operator induces elastic scattering between dark matter and gradients of the pNGB field, leading to momentum exchange without background energy transfer [8–10].

Following standard treatments of momentum-exchange IDE, we parametrize the drag force through an effective rate $\Gamma(a)$ appearing in the Euler equations [10, 28].

Dimensional analysis suggests $\Gamma \propto (c_6 v_s^2 / \Lambda^2 m_{DM}^2) \rho_{DM} H$, with proportionality constants of order unity depending on the details of the EFT matching. For computational implementation, we employ a simplified dimensionless parametrization

$$\frac{\Gamma(a)}{H(a)} \equiv \xi_{\text{eff}} f(a), \quad (22)$$

where ξ_{eff} is an effective coupling parameter that absorbs the microphysical coefficients c_6 , v_s , Λ , and m_{DM} , and $f(a)$ encodes the scale factor dependence. In our numerical exploration, we treat ξ_{eff} as a constant and vary it over a range corresponding to weak-to-moderate coupling, $\Gamma \lesssim \mathcal{O}(H)$. This captures the essential phenomenology of momentum-exchange IDE while maintaining perturbative control of the EFT.

The impact of the interaction on structure formation becomes significant when $\Gamma \sim H$ at late times, where dark energy perturbations are non-negligible and the drag term competes with Hubble friction in the dark matter Euler equation. As we demonstrate below, this leads to an asymptotic limit on the suppression of σ_8 that is insufficient to resolve the S_8 tension.

IV. RESULTS

We now present the numerical analysis of the Z_4 -IDSM cosmology, proceeding from the determination of the dark matter mass to the implications for large-scale structure. We first identify the parameter space yielding the observed dark matter relic density using `MicrOMEGAs` [29], then verify the radiative stability of the dark energy sector through renormalization group evolution, and finally implement the full cosmology in CLASS to assess the impact on the clustering amplitude σ_8 .

Viable Dark Matter Mass

The inert doublet mass m_{H_2} and the mass splitting between the neutral CP-even (H_2^0) and CP-odd (A_2^0) components are constrained by the requirement of obtaining the observed dark matter relic density, $\Omega_{\text{DM}} h^2 = 0.1199 \pm 0.0027$ [1]. We parameterize the mass degeneracy through $\delta = m_{A_2^0} - m_{H_2^0}$. In our model the CP-even candidate is the dark matter candidate and therefore is less massive than its CP-odd counterpart, so $\delta \geq 0$.

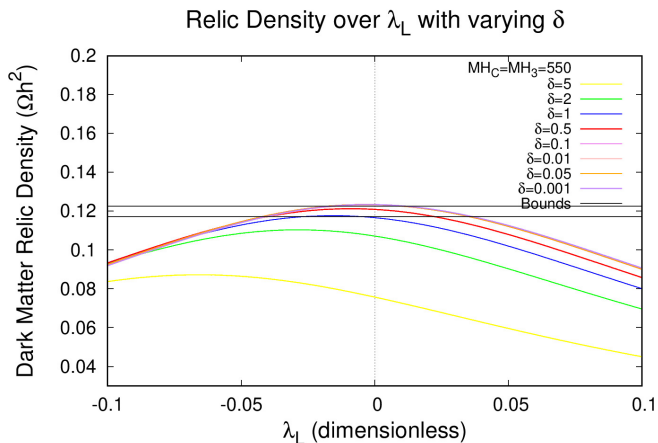


FIG. 1. Dark matter relic density $\Omega_{\text{DM}}h^2$ as a function of the Higgs portal coupling $\lambda_L = \lambda_3 + \lambda_4 + \lambda_5$ for various mass splittings δ , with $m_{H_2^0} = m_{H_2^\pm} = 550$ GeV. The horizontal bands indicate the Planck constraint $\Omega h^2 = 0.1199 \pm 0.0027$. Small splittings ($\delta \lesssim 1$ GeV) allow coannihilation effects to bring the relic density into the observed range.

Figure 1 shows the relic density as a function of λ_L for various δ . For large mass splittings ($\delta \gtrsim 1$ GeV), coannihilation is suppressed and the predicted relic density falls below the observed value unless $|\lambda_L| \gtrsim 0.05$. For small splittings ($\delta \lesssim 1$ GeV), coannihilation between H_2^0 , A_2^0 , and H_2^\pm efficiently depletes the thermal abundance, allowing agreement with Planck constraints within the perturbative regime $|\lambda_L| \lesssim 0.1$.

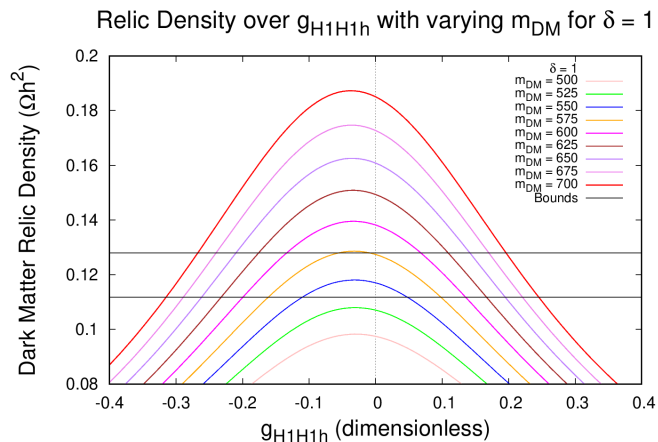


FIG. 2. Dark matter relic density as a function of the effective coupling $g_{H_1 H_1 h} = 2\lambda_L v$ [38] for $\delta = 1$ GeV and varying $m_{\text{DM}} \equiv m_{H_2^0}$. The horizontal bands indicate the Planck constraint. Heavier dark matter particles require larger portal couplings to achieve the observed relic density; the value $m_{\text{DM}} \approx 550$ GeV (blue curve) satisfies the Planck bound for natural couplings, consistent with results in the literature [39].

Figure 2 explores the m_{DM} dependence at fixed $\delta = 1$ GeV (for comparison with literature [39]). For $m_{\text{DM}} \lesssim 500$ GeV, the relic density is too low even for vanishing portal coupling due to large annihilation cross sections.

TABLE I. Renormalization group evolution of singlet mass parameters from the electroweak scale to $\Lambda = 10^8$ GeV for $\lambda_S = 0.5$. The hierarchy $|\mu_S^2|/|\mu_{sb}^2| \sim 10^{10}$ is preserved throughout.

Scale μ	$ \mu_S^2 $ [GeV ²]	$ \mu_{sb}^2 $ [GeV ²]	$ \mu_S^2/\mu_{sb}^2 $
$m_Z = 91$ GeV	2.5×10^{17}	1.0×10^{-84}	2.5×10^{101}
10^4 GeV	2.6×10^{17}	1.0×10^{-84}	2.6×10^{101}
10^8 GeV	3.0×10^{17}	1.2×10^{-84}	2.5×10^{101}

For $m_{\text{DM}} \gtrsim 600$ GeV, excessive overproduction requires $|\lambda_L| > 0.2$, approaching non-perturbative regimes. The optimal mass range $540 \lesssim m_{\text{DM}} \lesssim 560$ GeV yields the correct relic density for natural portal couplings.

Combining the constraints from both figures, we select

$$m_{\text{DM}} = 548 \text{ GeV} \quad (23)$$

corresponding to a nearly degenerate inert doublet with small but non-zero Higgs portal coupling.

Radiative Stability of Dark Energy

The radiative isolation of the dark energy sector is verified by evolving the mass parameters μ_S^2 and μ_{sb}^2 from the electroweak scale to the cutoff $\Lambda \sim 10^8$ GeV where the IDS_M loses perturbativity. We used the mathematica package called SARAH to compute the Renormalized Group Equations (RGEs). The one-loop RGEs receive no contributions from the Higgs or inert doublet sectors:

$$16\pi^2 \beta_{\mu_S^2} = 4\lambda_S \mu_S^2, \quad 16\pi^2 \beta_{\mu_{sb}^2} = 2\lambda_S \mu_{sb}^2. \quad (24)$$

Table I demonstrates this evolution for representative initial conditions with $\lambda_S = 0.5$. The hierarchy $|\mu_S^2| \sim v_s^2 \gg |\mu_{sb}^2| \sim H_0^2$ is preserved with less than 20% variation over the entire perturbative regime, confirming that the ultralight dark energy scale remains technically natural and is not destabilized by quantum corrections from the electroweak sector. The key feature is the absence of terms involving μ_1^2 , μ_2^2 , $\lambda_{3,4,5}$, or gauge/Yukawa couplings in Eqs. (24), ensuring the singlet sector evolves independently of the SM and dark matter parameters [22, 23].

Structure Formation and the S_8 Tension

We implement the momentum-exchange cosmology in CLASS using the parameters (23). Figure 3 shows the resulting clustering amplitude as a function of the dimensionless drag rate Γ/H , where we have absorbed the microphysics into the effective parameter ξ_{eff} encoding c_6 , v_s , Λ , and m_{DM} .

The pure Λ CDM baseline computed with our CLASS settings yields $\sigma_8^{\Lambda\text{CDM}} = 0.825$. When dark energy is treated as a dynamical fluid with equation of state $w(a)$

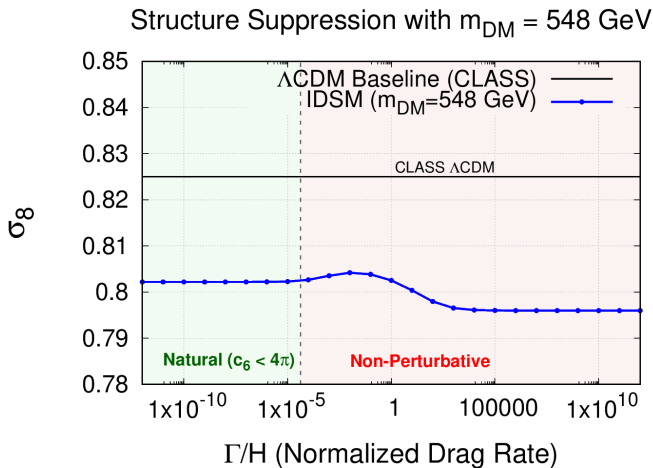


FIG. 3. Clustering amplitude σ_8 as a function of the normalized drag rate Γ/H for the Z_4 -IDSM with parameters (23). The horizontal black line shows the CLASS Λ CDM baseline $\sigma_8^{\Lambda\text{CDM}} = 0.825$. The green (red) shaded region indicates perturbative (non-perturbative) values of the EFT coupling c_6 . The IDSM prediction saturates at $\sigma_8 \approx 0.795$ for $\Gamma/H \gtrsim 10$.

and perturbations, but without momentum exchange ($\Gamma/H \rightarrow 0$), the baseline shifts to $\sigma_8 \approx 0.805$ due to the non-vanishing sound speed of the pNGB. As the drag rate increases, σ_8 initially exhibits mild enhancement before decreasing as momentum transfer suppresses structure growth. The suppression saturates at $\sigma_8 \approx 0.795$ for $\Gamma/H \gtrsim 10$.

The naturally achievable suppression in the perturbative regime ($c_6 \leq 4\pi$),

$$\frac{\sigma_8^{\text{IDSM}}}{\sigma_8^{\Lambda\text{CDM}}} \approx \frac{0.804}{0.825} \approx 0.974, \quad (25)$$

corresponds to a $\sim 2.6\%$ reduction in clustering amplitude, while the maximum achievable suppression in the strongly coupled regime,

$$\frac{\sigma_8^{\text{IDSM}}}{\sigma_8^{\Lambda\text{CDM}}} \approx \frac{0.795}{0.825} \approx 0.963, \quad (26)$$

yields $\sim 3.6\%$ reduction. Both fall short of the $\sim 5-10\%$ suppression required to resolve the S_8 tension [1, 3]. The saturation reflects a fundamental limitation: once $\Gamma \gtrsim H$, the dark sectors achieve velocity equilibrium and further coupling increases do not modify the growth history.

Our results demonstrate that symmetry-protected, momentum-exchange IDE scenarios possess an intrinsic ceiling on structure suppression. While theoretically controlled and free from background instabilities, they cannot—within their domain of validity—fully accommodate low-redshift cosmological data.

V. CONCLUSION

We have constructed a symmetry-protected framework for interacting dark energy in which dark matter and dark energy couple exclusively through momentum exchange. The Z_4 -IDSM model unifies two well-motivated extensions of the Standard Model: an inert scalar doublet stabilized by a discrete Z_4 symmetry provides the dark matter candidate, while a complex scalar singlet with softly broken global $U(1)_S$ yields a radiatively stable pseudo-Nambu-Goldstone boson for dark energy. This structure forbids renormalizable energy-transfer operators, ensuring background stability, while admitting a unique dimension-6 derivative interaction that generates observable effects on the growth of structure.

Our analysis reveals a fundamental tension in such constructions. The same symmetry structure that protects the ultralight dark energy scale from quantum corrections also suppresses the strength of dark sector interactions. We identified a viable dark matter candidate with $m_{\text{DM}} = 548$ GeV and demonstrated that the model achieves the observed relic density through coannihilation in the nearly-degenerate regime. Renormalization group evolution confirms that the singlet sector remains radiatively isolated from the electroweak scale, preserving the technical naturalness of the dark energy mass $m_\phi \sim H_0$.

However, when implemented in the Boltzmann code CLASS, the momentum-exchange interaction yields at most $\sim 3.6\%$ suppression of the clustering amplitude σ_8 relative to Λ CDM, saturating at $\sigma_8 \approx 0.795$ in the strong-coupling limit. This falls short of the $\sim 5-10\%$ reduction suggested by low-redshift observations. The saturation arises because momentum-exchange IDE efficiently equilibrates the dark sector velocities when $\Gamma \gtrsim H$, after which further increases in the coupling do not modify the growth history.

Several avenues remain for extending this framework. Introducing mild energy transfer through carefully tuned portal couplings could enhance structure suppression while maintaining background stability, though at the cost of reintroducing fine-tuning. Alternatively, generalizing the singlet sector to include multiple pNGBs or modifying the early-time dynamics through out-of-equilibrium effects may open new parameter space. More broadly, our results suggest that resolving the S_8 tension through dark sector interactions may require explicitly breaking the protective symmetries that render such models theoretically attractive, presenting a genuine dilemma for particle physics model-building.

The Z_4 -IDSM serves as a theoretically controlled benchmark: it demonstrates that even maximally symmetry-protected IDE scenarios face intrinsic limits on their observational impact. Future work must either identify mechanisms to circumvent these limits or confront the possibility that the S_8 tension originates from sources beyond the dark sector.

VI. APPENDIX

Appendix A: Renormalization Group Equations and Radiative Stability

The decoupling of the singlet sector is apparent from Table II: $\beta_{\mu_S^2}$ and $\beta_{\mu_{sb}^2}$ depend only on singlet self-couplings λ_S , with no contributions from Higgs/inert doublet parameters or SM gauge/Yukawa couplings. This confirms the radiative isolation essential for the technical naturalness of the dark energy scale.

1. Two-Loop Contributions

For completeness, we note that the evolution of the singlet mass parameters including two-loop effects takes the form:

$$\frac{d\mu_S^2}{dt} = \frac{1}{16\pi^2} \left[4\lambda_S\mu_S^2 - \frac{10\lambda_S^2\mu_S^2}{16\pi^2} \right], \quad (\text{A1})$$

$$\frac{d\mu_{sb}^2}{dt} = \frac{1}{16\pi^2} \left[2\lambda_S\mu_{sb}^2 - \frac{6\lambda_S^2\mu_{sb}^2}{16\pi^2} \right], \quad (\text{A2})$$

where the two-loop terms are suppressed by an additional factor of $16\pi^2$ and do not affect the qualitative conclusion of radiative stability.

2. Observation on Radiative Stability

As evidenced by the derived β -functions, the evolution of μ_S^2 and μ_{sb}^2 is entirely self-contained within the singlet sector. The absence of terms involving the SM Higgs mass (μ_1^2), electroweak gauge couplings (g_i), or the top Yukawa coupling (Y_u) confirms that the dark energy scale is technically natural. In this construction, the quintessence scale is protected from the Standard Model hierarchy problem, as no loop diagrams link the singlet mass to the ultraviolet-sensitive sectors of the SM.

Appendix B: Symmetry Structure and Technical Naturalness

The model's technical naturalness relies on a nested symmetry structure. We define the Z_4 group as the set of discrete rotations $\{1, \omega, \omega^2, \omega^3\}$ where $\omega = e^{i\pi/2}$.

The fields transform under Z_4 according to their assigned charges Q :

$$S \rightarrow \omega \cdot S = iS \quad (Q = 1), \quad (\text{B1})$$

$$H_2 \rightarrow \omega^2 \cdot H_2 = -H_2 \quad (Q = 2), \quad (\text{B2})$$

$$\text{SM Fields} \rightarrow \omega^0 \cdot \text{SM} = \text{SM} \quad (Q = 0). \quad (\text{B3})$$

The renormalizable potential is split into two parts based on their symmetry properties:

1. **The Z_4 -invariant sector:** Terms like $|S|^2$ and $|S|^4$ are invariant under the full group because the total charge sums to 0 (mod 4). This sector respects the global $U(1)_s$ and keeps the pNGB ϕ massless.
2. **The soft-breaking term:** We introduce the dimension-2 operator:

$$\mathcal{L}_{\text{soft}} \supset \frac{\mu_{sb}^2}{2}(S^2 + S^{\dagger 2}). \quad (\text{B4})$$

Under a Z_4 transformation $S \rightarrow iS$, the term transforms as $S^2 \rightarrow -S^2$. Since the Lagrangian is not invariant under the 90° rotation (ω), the Z_4 symmetry is explicitly broken.

Crucially, the S^2 term is invariant under the subgroup $Z_2 \subset Z_4$. If we apply the Z_4 transformation twice ($\omega^2 = -1$):

$$S \rightarrow -S \implies S^2 \rightarrow (-S)^2 = S^2. \quad (\text{B5})$$

This 180° rotation remains a valid symmetry of the full Lagrangian. Because H_2 carries a Z_4 charge of 2, it also transforms under this residual Z_2 as:

$$H_2 \xrightarrow{Z_2} -H_2. \quad (\text{B6})$$

This ensures that H_2 (the dark matter) is the lightest parity-odd particle under the surviving Z_2 . Since all Standard Model particles are even under Z_2 , the stability of dark matter is mathematically guaranteed despite the mass-generating break in the singlet sector.

1. Technical Naturalness and Dimensional Analysis

The stability of the dark energy scale $\mu_{sb}^2 \ll v^2$ is guaranteed by the ‘‘soft’’ nature of the breaking term. In quantum field theory, the sensitivity of the vacuum to radiative corrections is governed by the dimensionality of the operators.

The term $V_{\text{soft}} = \frac{\mu_{sb}^2}{2}(S^2 + S^{\dagger 2})$ is a mass-dimension 2 operator. Its contribution to the renormalization group equations of the dimensionless couplings λ_i is identically zero at the renormalizable level:

$$\frac{d\lambda_i}{d \ln \mu} \propto \mathcal{F}(\lambda_j, g_k, y_l) \neq \mathcal{G}(\mu_{sb}^2). \quad (\text{B7})$$

Because dimensionless couplings cannot depend linearly on mass-squared parameters (due to dimensional consistency), the smallness of the dark energy scale does not ‘‘pollute’’ the stability of the Higgs quartic coupling or the gauge sector.

According to 't Hooft's prescription, a parameter is technically natural if setting it to zero increases the symmetry of the theory [21]:

- If $\mu_{sb}^2 \rightarrow 0$, the potential gains an exact $U(1)_s$ and Z_4 symmetry.

TABLE II. One-loop renormalization group equations for the Z_4 -IDSM model. Yukawa couplings are shown for a single generation.

Parameter	$\beta^{(1)} \times 16\pi^2$
g_1	$\frac{21}{10}g_1^3$
g_2	$-3g_2^3$
g_3	$-7g_3^3$
μ_1^2	$-\frac{9}{10}g_1^2\mu_1^2 - \frac{9}{2}g_2^2\mu_1^2 + 6\lambda_1\mu_1^2 + 4\lambda_3\mu_2^2 + 2\lambda_4\mu_2^2 + 6\mu_1^2\text{Tr}(Y_u^2 + Y_d^2) + 2\mu_1^2\text{Tr}(Y_e^2)$
μ_2^2	$4\lambda_3\mu_1^2 + 2\lambda_4\mu_1^2 - \frac{9}{10}g_1^2\mu_2^2 - \frac{9}{2}g_2^2\mu_2^2 + 6\lambda_2\mu_2^2$
μ_S^2	$4\lambda_S\mu_S^2$
μ_{sb}^2	$2\lambda_S\mu_{sb}^2$
Y_u	$Y_u[\frac{3}{2}(Y_u^2 - Y_d^2) + 3\text{Tr}(Y_u^2 + Y_d^2) + \text{Tr}(Y_e^2) - \frac{17}{20}g_1^2 - \frac{9}{4}g_2^2 - 8g_3^2]$
Y_d	$Y_d[\frac{3}{2}(Y_d^2 - Y_u^2) + 3\text{Tr}(Y_u^2 + Y_d^2) + \text{Tr}(Y_e^2) - \frac{1}{4}g_1^2 - \frac{9}{4}g_2^2 - 8g_3^2]$

- If the portal couplings $\lambda_{S1}, \lambda_{S2} \rightarrow 0$, the singlet sector becomes completely decoupled from the SM.

Thus, the tiny value of μ_{sb}^2 is protected from large corrections by the fact that it is the *unique* source of symmetry breaking in the singlet sector. Any radiative correction to μ_{sb}^2 must be proportional to μ_{sb}^2 itself, ensuring that once it is set small, it remains small at all scales [22, 23].

Appendix C: Detailed Derivation of the Singlet Sector Mass Spectrum

We derive the tree-level masses for the radial mode ρ and the pseudo-Nambu-Goldstone boson (pNGB) ϕ . We consider the singlet scalar potential:

$$V_S = \mu_S^2 |S|^2 + \frac{\lambda_S}{2} |S|^4 + \frac{\mu_{sb}^2}{2} (S^2 + S^{\dagger 2}), \quad (\text{C1})$$

where S is expanded around its vacuum expectation value v_s as:

$$S = \frac{v_s + \rho + i\phi}{\sqrt{2}}. \quad (\text{C2})$$

1. Field Expansion

$$|S|^2 = SS^\dagger = \frac{1}{2}(v_s + \rho + i\phi)(v_s + \rho - i\phi) = \frac{1}{2}[(v_s + \rho)^2 + \phi^2]. \quad (\text{C3})$$

Expanding this gives:

$$|S|^2 = \frac{1}{2}v_s^2 + v_s\rho + \frac{1}{2}\rho^2 + \frac{1}{2}\phi^2. \quad (\text{C4})$$

We square the result from the previous step, keeping only terms up to quadratic order in the fields (as cubic and quartic terms do not contribute to tree-level masses):

$$\begin{aligned} |S|^4 &= \left(\frac{1}{2}v_s^2 + v_s\rho + \frac{1}{2}\rho^2 + \frac{1}{2}\phi^2 \right)^2 \\ &\approx \frac{1}{4}v_s^4 + v_s^3\rho + \frac{3}{2}v_s^2\rho^2 + \frac{1}{2}v_s^2\phi^2. \end{aligned} \quad (\text{C5})$$

$$\begin{aligned} S^2 + S^{\dagger 2} &= \frac{1}{2}(v_s + \rho + i\phi)^2 + \frac{1}{2}(v_s + \rho - i\phi)^2 \\ &= (v_s + \rho)^2 - \phi^2 \\ &= v_s^2 + 2v_s\rho + \rho^2 - \phi^2. \end{aligned} \quad (\text{C6})$$

2. The Potential at Quadratic Order

Substituting these expansions back into V_S , we isolate the constant (vacuum), linear (tadpole), and quadratic (mass) pieces:

$$\begin{aligned} V_S \supset \rho &\left[v_s\mu_S^2 + \frac{\lambda_S}{2}v_s^3 + v_s\mu_{sb}^2 \right] \\ &+ \frac{1}{2}\rho^2 \left[\mu_S^2 + \frac{3}{2}\lambda_S v_s^2 + \mu_{sb}^2 \right] \\ &+ \frac{1}{2}\phi^2 \left[\mu_S^2 + \frac{1}{2}\lambda_S v_s^2 - \mu_{sb}^2 \right]. \end{aligned} \quad (\text{C7})$$

3. Vacuum Extremization and Tadpole Cancellation

For the vacuum to be stable, the linear term in ρ (the tadpole) must vanish:

$$\frac{\partial V}{\partial \rho} = 0 \implies v_s \left(\mu_S^2 + \mu_{sb}^2 + \frac{\lambda_S}{2}v_s^2 \right) = 0. \quad (\text{C8})$$

Assuming $v_s \neq 0$, we obtain the critical tadpole relation:

$$\mu_S^2 + \frac{\lambda_S}{2}v_s^2 = -\mu_{sb}^2. \quad (\text{C9})$$

4. Final Mass Eigenvalues

We now substitute the tadpole relation (C9) into the quadratic coefficients to find the physical masses squared $m^2 = \partial^2 V / \partial \varphi^2$.

Radial mode ρ :

$$m_\rho^2 = \mu_S^2 + \mu_{sb}^2 + \frac{3}{2}\lambda_S v_s^2 \\ = \left(-\frac{\lambda_S}{2}v_s^2 - \mu_{sb}^2\right) + \mu_{sb}^2 + \frac{3}{2}\lambda_S v_s^2 = \lambda_S v_s^2. \quad (\text{C10})$$

p NGB mode ϕ :

$$m_\phi^2 = \mu_S^2 - \mu_{sb}^2 + \frac{1}{2}\lambda_S v_s^2 \\ = \left(-\frac{\lambda_S}{2}v_s^2 - \mu_{sb}^2\right) - \mu_{sb}^2 + \frac{1}{2}\lambda_S v_s^2 = -2\mu_{sb}^2. \quad (\text{C11})$$

Taking the convention where $\mu_{sb}^2 < 0$, we define $m_\phi^2 = 2|\mu_{sb}^2|$, which completes the derivation.

-
- [1] N. Aghanim *et al.* (Planck Collaboration), “Planck 2018 results. VI. Cosmological parameters,” *Astron. Astrophys.* **641**, A6 (2020).
- [2] A. G. Riess *et al.*, “A Comprehensive Measurement of the Local Value of the Hubble Constant,” *Astrophys. J. Lett.* **934**, L7 (2022).
- [3] DESI Collaboration, “DESI 2024 Results: Cosmological Constraints from the First Year of Data,” arXiv:2404.03002.
- [4] L. Amendola, “Coupled quintessence,” *Phys. Rev. D* **62**, 043511 (2000).
- [5] C. Wetterich, “The Cosmon model for an asymptotically vanishing time dependent cosmological constant,” *Astron. Astrophys.* **301**, 321 (1995).
- [6] J. Valiviita, E. Majerotto and R. Maartens, “Instability in interacting dark energy and dark matter fluids,” *JCAP* **07**, 020 (2008).
- [7] J.-H. He, B. Wang and P. Zhang, “The imprint of the interaction between dark sectors in large scale cosmic microwave background anisotropies,” *Phys. Rev. D* **80**, 063530 (2009).
- [8] F. Simpson, “Scattering of dark matter and dark energy,” *Phys. Rev. D* **82**, 083505 (2010).
- [9] A. Poursidou, C. Skordis and E. J. Copeland, “Models of dark matter coupled to dark energy,” *Phys. Rev. D* **88**, 083505 (2013).
- [10] C. Skordis, A. Poursidou and E. J. Copeland, “Parametrized post-Friedmann framework for interacting dark energy,” *Phys. Rev. D* **91**, 083537 (2015).
- [11] S. M. Carroll, “Quintessence and the rest of the world,” *Phys. Rev. Lett.* **81**, 3067 (1998).
- [12] N. Kaloper and A. Padilla, “Vacuum Energy Sequestering and Gravitational Radiative Stability,” *Phys. Rev. Lett.* **114**, 101302 (2015).
- [13] J. A. Frieman, C. T. Hill, A. Stebbins and I. Waga, “Cosmology with ultralight pseudo Nambu-Goldstone bosons,” *Phys. Rev. Lett.* **75**, 2077 (1995).
- [14] K. Choi, “String or M theory axion as a quintessence,” *Phys. Rev. D* **62**, 043509 (2000).
- [15] N. G. Deshpande and E. Ma, “Pattern of symmetry breaking with two Higgs doublets,” *Phys. Rev. D* **18**, 2574 (1978).
- [16] R. Barbieri, L. J. Hall and V. S. Rychkov, “Improved naturalness with a heavy Higgs: An Alternative road to LHC physics,” *Phys. Rev. D* **74**, 015007 (2006).
- [17] M. Gustafsson, E. Lundstrom, L. Bergstrom and J. Edsjo, “Significant gamma lines from inert Higgs dark matter,” *Phys. Rev. Lett.* **99**, 041301 (2007).
- [18] G. Bélanger, A. Mjallal and A. Pukhov, “The case of inert doublet and singlet scalars,” *Phys. Rev. D* **105**, 035018 (2022).
- [19] G. Bélanger, K. Kannike, A. Pukhov and M. Raidal, “Multi-component dark matter with a magnetic dipole and a Z_4 symmetry,” *JCAP* **01**, 027 (2012).
- [20] J. Kim, S.-S. Kim, H. M. Lee and R. Padhan, “Small Neutrino Masses from a Decoupled Singlet Scalar Field,” arXiv:2407.13595 [hep-ph] (2024).
- [21] G. ’t Hooft, “Naturalness, chiral symmetry, and spontaneous chiral symmetry breaking,” in *Recent Developments in Gauge Theories*, NATO Adv. Study Inst. Ser. B Phys. **59**, 135 (1980).
- [22] G. F. Giudice, “Naturally Speaking: The Naturalness Criterion and Physics at the LHC,” arXiv:0801.2562 [hep-ph] (2008).
- [23] M. D. Schwartz *et al.*, “Snowmass 2021 White Paper: Naturalness,” arXiv:2205.05708 [hep-ph] (2022).
- [24] P. J. E. Peebles and B. Ratra, “Cosmology with a Time-Variable Cosmological Constant,” *Astrophys. J.* **325**, L17 (1988).
- [25] S. R. Coleman and E. J. Weinberg, “Radiative Corrections as the Origin of Spontaneous Symmetry Breaking,” *Phys. Rev. D* **7**, 1888 (1973).
- [26] S. Weinberg, “The Cosmological Constant Problem,” *Rev. Mod. Phys.* **61**, 1 (1989).
- [27] S. Weinberg, “Phenomenological Lagrangians,” *Physica A* **96**, 327 (1979).
- [28] J. Linton, R. Crittenden and A. Poursidou, “Momentum transfer models of interacting dark energy,” *JCAP* **08**, 075 (2022).
- [29] G. Bélanger, F. Boudjema, A. Pukhov, A. Semenov, micrOMEGAs: A tool for dark matter studies, *Comput. Phys. Commun.* **182**, 842 (2011). <https://arxiv.org/abs/1005.4133>
- [30] G. Bélanger *et al.*, micrOMEGAs5.0: Freeze-in, *Comput. Phys. Commun.* **231**, 173 (2018). <https://arxiv.org/abs/1801.03509>
- [31] J. Lesgourgues and T. Tram, “The Cosmic Linear Anisotropy Solving System (CLASS) I: Overview,” (2011). <https://arxiv.org/abs/1104.2932>
- [32] D. Blas, J. Lesgourgues and T. Tram, “The Cosmic Linear Anisotropy Solving System (CLASS) II: Approximation schemes,” *JCAP* **07**, 034 (2011) [arXiv:1104.2933 [astro-ph.CO]].
- [33] W. Hu and I. Sawicki, “A Parameterized Post-Friedmann Framework for Modified Gravity,” *Phys. Rev. D* **76**, 104043 (2007) [arXiv:0708.1190 [astro-ph]].
- [34] W. Fang, W. Hu and A. Lewis, “Crossing the Phantom Divide with Parameterized Post-Friedmann Dark Energy,” *Phys. Rev. D* **78**, 087303 (2008) [arXiv:0808.3125 [astro-ph]].
- [35] H. Kodama and M. Sasaki, “Cosmological Perturbation Theory,” *Prog. Theor. Phys. Suppl.* **78**, 1 (1984).

- [36] C.-P. Ma and E. Bertschinger, “Cosmological Perturbation Theory in the Synchronous and Conformal Newtonian Gauges,” *Astrophys. J.* **455**, 7 (1995) [arXiv:astro-ph/9506072].
- [37] G. Benevento, M. Ballardini, M. Braglia and F. Finelli, “Matter power spectrum in a CLASS of alternative dark energy models: comparative analysis of the baryon acoustic oscillation measurements,” *JCAP* **04**, 041 (2020) [arXiv:1911.06064 [astro-ph.CO]].
- [38] L. Lopez Honorez, E. Nezri, J. F. Oliver and M. H. G. Tytgat, “The inert doublet model: An archetype for dark matter,” *JCAP* **0702**, 028 (2007).
- [39] Venus Keus, Stephen F. King, Stefano Moretti, and Dorota Sokolowska, *Observable heavy Higgs dark matter*, *Journal of High Energy Physics*, 2015(11):3, 2015.
- [40] J. Lee, S. Lee and J. Kim, “ $N = 2$ PANGB Quintessence Dark Energy,” *J. Korean Phys. Soc.* **79**, 336 (2021) [arXiv:2002.01756 [astro-ph.CO]].
- [41] N. Cruickshank, R. Crittenden and A. Pourtsidou, “Forecasts for interacting dark energy with time-dependent momentum exchange,” arXiv:2504.03555 [astro-ph.CO] (2025).